Heliyon 6 (2020) e04575

Contents lists available at ScienceDirect

Heliyon

journal homepage: www.cell.com/heliyon

Research article

Advanced nanoindentation simulations for carbon nanotube reinforced nanocomposites

Khondaker Sakil Ahmed [a,*], Ibriju Ibrahim [a], Ang Kok Keng [b]

[a] Department of Civil Engineering, Military Institute of Science and Technology, Dhaka, 1216, Bangladesh
[b] Department of Civil and Environmental Engineering, National University of Singapore, 1, Engineering Drive 2, 117576, Singapore

ARTICLE INFO

Keywords:
Nanotechnology
Structural engineering
Carbon nanotube
Non-bonded interface
Nanocomposite
Wall thickness dependency
Nanoindentation

ABSTRACT

Mechanical properties of Carbon Nanotube (CNT) reinforced composites are obtained utilizing finite element (FE) method-based indentation simulations considering large strain elasto-plastic behavior of elements. This study includes nanoindentation simulations for chemically non-bonded CNT/matrix interface, including the length scale effect of nanocomposites. In order to investigate the mechanical properties of CNT reinforced nanocomposites, a number of FE models for nanoindentation tests have been simulated. Sample nanocomposites are examined to determine the suitable types of CNTs and their effectiveness as a reinforcement of different potential matrices. The Parametric study is conducted to obtain the influence of wall thickness, relative positioning, and volume fraction of CNT and strain hardening parameter of matrix on the mechanical properties of nanocomposites. The obtained results indicate that, properties such as modulus of elasticity and hardness of the nanocomposites are largely dependent on wall thickness of CNT and strain hardening parameter of the matrix. This study also suggests, the minimum wall thickness of CNT to avoid local buckling in nanocomposite which is required to be at least 0.2 nm for a diameter to thickness ratio of 5.0. Moreover, a matrix having a value of strain hardening parameter near 0.1 is expected to be significantly effective for nanocomposite.

1. Introduction

Carbon nanotubes are considered as the key reinforcing element of high-performance nanocomposites [1, 2, 3, 4, 5, 6]. Existing research suggests that the load carrying ability of composites can be improved significantly by the addition of carbon nanotubes or nano-ropes [4, 7, 8]. Chen et al (2004) observed in his study that an addition of 3.6% CNTs by volume in a matrix, the tensile stiffness of the nanocomposites can be increased by as much as 33% [4]. Mechanical properties such as modulus of elasticity and hardness of nanocomposites, are some of the important features that are indispensable to determine before their application. However, mechanical properties of many CNT based nanocomposites are yet to be determined, as difficulty arises in measuring force components or stresses and strains at nano-scale through experimental investigation. Therefore, it becomes more viable alternative approach to predict these mechanical properties using numerical methods for nanocomposites for which experimental set-up is not only quite difficult to arrange but also expensive and sometimes nearly impossible. Nanoindentation test using numerical model is one of the approaches that is capable of determining mechanical properties of such nanocomposites using indentation model quite accurately [9, 10, 11, 12].

Atomistic simulations for CNT based nanocomposites are mainly founded on molecular dynamic (MD) and molecular mechanics (MM) simulations or density functional theory (DFT) which are widely acknowledged for their accuracies in result predictions [13, 14, 15, 16, 17]. The main attention of these studies was to understand the effect of different types of bonding at the CNT/matrix interface such as covalent, non-covalent van der Waals forces or electrostatic forces and the influence of friction at the CNT/matrix interface. MM and MD simulations are usually performed with certain limitations such as small domain, constant number of atoms, and constant temperature, and pressure. In order to overcome such difficulty, some researchers effectively employed multiscale and multi-surface constitutive model on polymer matrix [18]. Micromechanical models are another promising method for nanocomposites and such approach gains popularity to investigate mechanical properties of nanocomposites because of their computational effectiveness [19, 20, 21, 22]. Creep, thermo mechanical and electrical conductivity of nanocomposites were also investigated using similar analytical formulations [23, 24, 25]. They observed that when uniform dispersion

* Corresponding author.
E-mail address: drksa@ce.mist.ac.bd (K.S. Ahmed).

https://doi.org/10.1016/j.heliyon.2020.e04575
Received 16 March 2020; Received in revised form 19 May 2020; Accepted 24 July 2020

of CNTs are used, most accurate creep response is observed. Performance of these methods may be considered as improved level since they produce a better computational competence of larger volume of nanocomposite compare to that of MD simulations.

Experimental set-up for depth sensing indentation procedure was first successfully tested and developed by Doerner and Nix (1986) [26]. The determination of modulus of elasticity of any solid materials using finite element based indentation analysis was originally proposed by Larsson et al. (1996) [12]. Later, nano-indentation test on polymeric surface was primarily conducted by Briscoe et al. (1998) [27]. Based on the indentation technique, Fazio et al. (2001) conducted nano-indentation tests for diamond and hence results were also compared with their finite element model [10]. Indentation test for carbon nanotube based composites has been studied since 2003 [11,28-33]. Research study on graphene fibre reinforced composite using indentation analysis was conducted by Barun et al. (2009) [34]. Experimental nanoindentation is employed on cu composites reinforced by graphene nano platelets [35]. Further advancement was made when hybrid CNTS such as MWCNTS, graphene-oxide nanotubes reinforced acrylonitrile butadiene styrene (ABS) nanocomposites were studied using experimental nanoindentation to examine micro hardness and modulus of elasticity of nanocomposite by Jyoti et al. (2018) [36]. Recently, experimental nanoindentation on graphene and MWCNT based composite conducted by Batakliev et al. [37] revealed that nano fillers improves the mechanical properties of poly lactic acid (PLA) based nanocomposites. Previous research on indentation analysis therefore suggests that indentation simulation using finite element analysis allows comprehensive understanding of the progression of deformation in the contact regions and also the stress transferring mechanism in the solid medium. Though all these studies enormously contribute in determining the mechanical properties of solids and polymers, none of those studies accounts for the issues related to length scale effect of CNTs and nanocomposites which is predominant more particularly when the sizes of the constituents are in micro or nano scale.

Harsono et al. (2009) [38] successfully estimated the material characterization including the incorporation of size effect of polymeric material with strain gradient plasticity, which was actually an extension of a previous work conducted by van Melick et al. (2003) [9]. Furthermore, study on size effect on thin film for micron to sub-micron level was also conducted by Borrero et al. (2009) [39]. All of these studies on “size effect” ensure that there is strong size dependency on mechanical properties of the materials on micron to nano-scale. In fact, they have considered the size effect using strain gradient plasticity which is more appropriate to account the material characterization at micro or nano scale. Such contributions certainly create significant interests of research on capturing size effect issue for micro to nanocomposites.

A good number of research studies recommended that the strength and stiffness of CNT reinforced nanocomposites largely depends on the CNT/matrix interface and chemical bonding or non-bonding at the interface play a major role on the mechanical properties of nanocomposites [7, 8, 17, 40, 41, 42, 43, 44, 45, 46]. Msekh et. al. (2018) proposed a phase field approach to model fracture of nano silicate clay composite. Their model reveals that the interface parameters influence the tensile strength and fracture parameters of composites [47]. Previously, Talebi et. al. (2013) proposed a computational library and developed an open source software using extended finite element methods for investigating nanocomposites. Their framework can be used for atomistic-continuum coupling with either concurrent or semi-concurrent methods [48]. Recently, a number of studies are conducted on indentation analysis using finite element method for material characterization of carbon nanotube reinforced composite [31, 49]. However, their studies consider perfectly bonded CNT/matrix interface for nanocomposites which is practically possible by creating covalent bonding at the interface. In addition, the later study on SWCNT reinforced composite has been conducted at micro scale (indentation depth 5 μm) model which is not capable to incorporate material size effect. However, chemical bonding or perfect interface is very difficult to achieve for nanocomposites. Additionally, in many cases it's not possible to find long and defect-free CNTs that ultimately results a non-bonded CNT/matrix interface inside the composite. In such situation, non-bonded interface is very essential to consider in modeling of nanocomposites and hence its influence on mechanical properties of nanocomposites are very important to investigate before their practical application.

This study aims to investigate the mechanical properties of CNT reinforced nanocomposites using FE based indentation simulation with strain gradient plasticity to incorporate the size effect for non-bonded carbon nanotube in the matrix. With a view to relate with more practical scenario of a non-bonded interface, this study includes mechanical interlocking as friction, thermal stress due to initial processing temperature and vdW interactions at the CNT/matrix interface. The study also investigates the behavior of different CNTs and their effectiveness as reinforcement in both polymeric resin and metal matrix nanocomposites. The detail indentation analysis also includes the parametric study to obtain the influence of wall thickness, volume fraction, nanotube's relative position with the indenter and strain hardening coefficient dependencies on mechanical properties of CNT based nanocomposites. This new approach would be a breakthrough to model nanoindentation test at nanoscale using advanced finite element method and hence predict the material properties of nanocomposites before their practical applications.

2. Numerical modeling procedure & formulation

In order to develop an accurate finite element model that is capable of capturing length scale effect with strain gradient plasticity for a non-bonded CNT/matrix interface, a set of theories and formulations have been followed to create a program and hence run the Finite Element (FE) model by FE software abaqus v14.1.

2.1. Incorporation of length scale and plasticity in finite element model

The relationship between the total dislocation density plasticity and shear flow stress can be expressed based on Taylor dislocation model (1934) as [50].

$$\tau = \alpha G b \sqrt{\rho_S} + \rho_G \tag{1}$$

where

b the magnitude of the Burger's vector

G the shear modulus

α the value this empirical constant is 0.2–0.5 depending on the type of materials

M is termed as the Taylor Factor that relates between the tensile yield strength (σ_f) and shear strength (τ) of the materials. Therefore, the relationship between them may be expressed as

$$\sigma_f = M \times \tau \tag{2}$$

M = 3.06 for face-cantered-cubic materials [51].

The tensile flow stress (σ_f) is representing the stress plastic strain curve of uniaxial tension as

$$\sigma_f = M\alpha G b \sqrt{\rho_s} = \sigma_Y f(\varepsilon^P) \tag{3}$$

After rearranging Eq. (3),

$$\rho_s = \left[\sigma_Y f(\varepsilon^P)\big/ M\alpha G b\right]^2 \tag{4}$$

Ashby (1970) [52] modified the expression for the density of geometrically necessary dislocations (ρ_G) and proposed the following equation

$$\rho_G = \frac{\bar{r}\eta^P}{b} \tag{5}$$

η^P the effective strain gradient due to plasticity

$\bar{r}$ Nye factor, reflecting the appropriate contribution of geometrically necessary dislocation density. The values of the factor are 1.85 for bending and 1.93 for torsion for face-centered-cubic materials [53].

In view of Eq. (3), Eq. (4) and Eq. (5), the flow stress derived from the Taylor's dislocation model may be expressed as

$$\sigma_f = M_\tau = M\alpha Gb\sqrt{\rho_s} + \rho_G \tag{6}$$

After rearranging and simplification, Eq. (6) may be rewritten as

$$\sigma_f = \sigma_Y\sqrt{f^2(\varepsilon^P) + I\eta^2} \tag{7}$$

where, I is termed as the material length scale which can be expressed as

$$I = M^2\alpha^2\left(\frac{G}{\sigma_Y}\right)^2 b \tag{8}$$

The estimated values of the inherent material length scale are generally obtained in the order of fraction of micron or a fraction of micron. In view of the visco-plastic limit proposed by Kok et al. (2002), the power law for visco plastic material can be expressed as [54].

$$\varepsilon^P = \dot{\varepsilon}\left[\frac{\sigma_e}{\sigma_Y f(\varepsilon^P)}\right]^2 \tag{9}$$

$$\dot{\varepsilon} = \sqrt{\frac{2}{3}\dot{\varepsilon}^\tau_{ij}\dot{\varepsilon}^\tau_{ij}} \tag{10}$$

$$\dot{\varepsilon}^\tau_{ij} = \dot{\varepsilon}_{ij} - \frac{1}{3}\dot{\varepsilon}_{kk}\delta_{ij} \tag{11}$$

$\dot{\varepsilon}$ the effective strain rate
m the rate sensitivity exponent
$\dot{\varepsilon}^\tau_{ij}$ the deviatoric strain rate
σ_e the effective von Mises stress
σ_Y the initial yield stresses

The stress to plastic strain relation for a power law hardening solids is expressed as

$$\sigma_Y f(\varepsilon^P) = \sigma_Y\left(1 + \frac{\varepsilon^P}{\varepsilon_Y}\right)^n \tag{12}$$

where, n is the plastic work hardening exponent or may be termed as strain hardening parameter, the value of which varies from 0.0 to 0.6. A separate parametric study has been conducted to examine the influence of this parameter on the nanocomposites.

Replacing the uni-axial flow stress by the flow stress and further incorporating the strain gradient effects, the plastic strain rate takes the following form

$$\dot{\varepsilon}^P = \dot{\varepsilon}\left[\frac{\sigma_e}{\sigma_f}\right]^m = \dot{\varepsilon}\left[\frac{\sigma_e}{\sigma_Y\sqrt{f^2(\varepsilon^P) + I\eta^P}}\right]^m \tag{13}$$

where,

η^P the effective plastic strain gradient

The constitutive relationship expressed as strain rate encompasses the elastic and plastic components of strain rate as

$$\dot{\varepsilon}_{ij} = \dot{\varepsilon}^e_{ij} + \dot{\varepsilon}^p_{ij} \tag{14}$$

The elastic strain rate may be obtained from bulk modulus, the stress rate as presented

$$^*\dot{\varepsilon}^e_{ij} = \frac{1}{2\mu}\dot{\sigma}^{'}_{ij} + \frac{\dot{\sigma}_{kk}}{9K}\delta_{ij} \tag{15}$$

where,

K is the bulk modulus
$\sigma_{kk} = (\sigma_{11} + \sigma_{22} + \sigma_{33})$

$\dot{\sigma}^{'}_{ij}$ is the deviatoric stress rate that can be expressed as

$$\dot{\sigma}^{'}_{ij} = \dot{\sigma}_{ij} - \frac{\dot{\sigma}_{kk}\delta_{ij}}{3} \tag{16}$$

2.2. Finite element model

In this study, an axisymmetric finite element model has been developed primarily to conduct numerical indentation test as shown in Figure 1. The figure presents a representative FE model single-wall carbon nanotube (SWCNT) and multi-wall carbon nanotube (MWCNT) reinforced nanocomposites. The inclination angles of the faces with respect to the loading axis were 65.3^0 for Berkovich indenter. Later, the model is reproduced for model validation and parametric studies using the same concept.

The basic finite element modeling assumptions include that nanotubes and matrix are defect free, homogeneous and isotropic. CNTs are hollow, cylindrical in shape and straight. The dispersion of CNTs are approximated to be uniform in the matrix. The plasticity and length scale effect of the constituents are captured by strain gradient plasticity as described in subsection 2.1. The interface between CNTs and matrix is a frictional interface where thermal residual stress, mechanical interlocking and vdW interactions (i.e. there is no chemical bonding between them) control the interface strength. Both material and geometric nonlinearity are considered in the analysis procedure.

The domain size of the axisymmetric model is 10nm by 10nm that results a total $100nm^2$. A total nine numbers of equal size CNTs presents in the model with an outer diameter 1nm. For SWCNT, the wall thickness is used to be 0.034nm and the thickness of the nanotube increases as per number of layers. 8-node quadrilateral solid elements are employed for appropriate meshing of the model. In the model, very fine meshes are selected using mesh sensitivity analysis so that FE models can be analyzed more accurately by providing minimum analysis run time for models. Mesh biasness in different zones of the model is also considered. In view of biasness, more number of elements by reducing element sizes are chosen near the indenter tip to make the analysis more efficient so that desired convergence of output can be achieved. Total number of elements in each side adjacent to indenter tip is 100 with a bias ratio of 1:10. The finite element model contains a total number of 18917 and 20213 elements for SWCNT and MWCNT reinforced composites, respectively. A total 17099 elements are from matrix and 1818 elements from SWCNTs (202 elements for each SWCNTs). Each MWCNT contains 346 solid elements that makes a total 3114 for nine MWCNTs in matrix.

The boundary condition at the bottom side of the matrix is considered to be restrained in Y direction (U2 = 0) and the left side of the model is restrained in X direction (U1 = 0 and UR3 = 0). Stress stain relationship for CNTs are adopted from the study conducted by Wernik et. al. (2010) [55]. As interaction, the indenter is considered to be analytically rigid. Surface to surface interaction between CNT and matrix is considered to be friction for non-bonded interface where matrix is the master surface and CNT the slave. In the non-bonded interface, thermal stress is considered as uniform radial pressure acting on the nanotube. The details of non-bonded interface is described in section 2.3. A study on parameter dependencies are also performed to determine the influence of wall thickness, volume fractions, relative nanotube position and strain hardening parameters.

2.3. Modeling of non-bonded interface

All the previous studies on indentation simulation of CNT based nanocomposites considered perfect interface between the CNTs and matrix. The modeling of CNT/matrix non-bonded interface using FE simulations becomes tricky and complicated. The formulation becomes even more complex when size effect is incorporated with vdW interaction for the non-bonded CNT/matrix interface. This study considers frictional

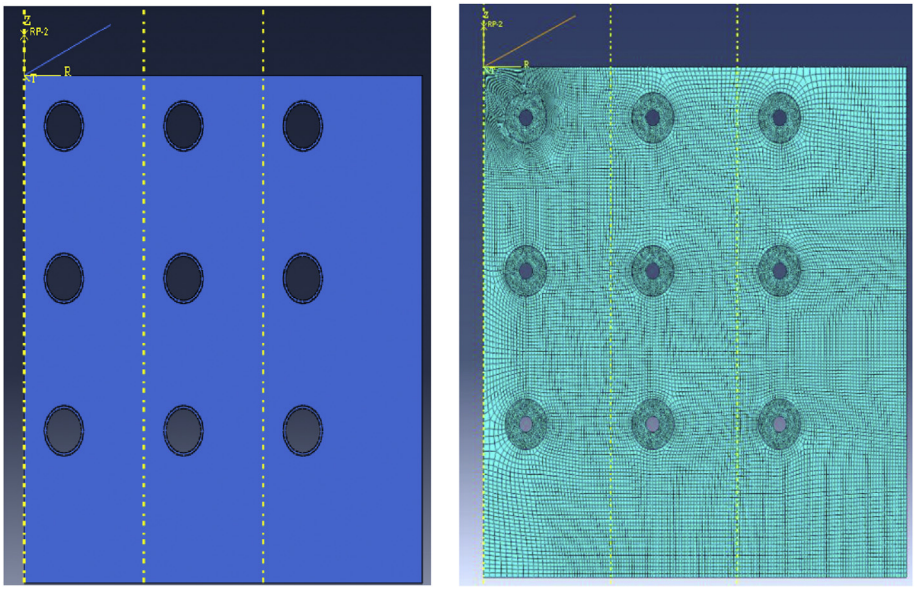

Figure 1. Finite element model of CNT reinforced nanocomposites; a. SWCNT (without meshing) in matrix, b. MWCNT reinforced nanocomposite.

interface to represent the mechanical interlocking between CNT and matrix. This frictional non-bonded interface is composed by residual stress due to thermal mismatch, mechanical interlocking and vdW interactions.

2.3.1. Approximation of thermal residual stress

A radial residual stress is produced at the CNT/matrix interface that generally develops from the matrix shrinkage due to differential thermal contraction upon cooling from the processing temperature. This radial stress acts as a uniform pressure over the entire interface, which can be estimated directly through individual material properties. This uniform radial stress (q_{res}) has been determined to be function of thermal contraction, temperature change, Poisson's ratio, volume fraction, and modulus of elasticity of the constituents as follows [56].

$$q_{res} = \frac{\frac{E_m\gamma_m}{2}\left[1+\nu_t+\frac{(\nu_m-\nu_t)\gamma_t E_t}{E}\right](\alpha_t-\alpha_m)\Delta T}{\left\{1-\frac{\left(1-\frac{E_m}{E_t}\right)(1-\nu_t)}{2}+\frac{\gamma_m(\nu_m-\nu_t)}{2}-\left(\frac{E_m}{E_t}\right)\left[\nu_t+\frac{(\nu_m-\nu_t)\gamma_t E_t}{E}\right]^2\right\}} \tag{17}$$

whereΔT is the temperature difference after thermal cooling;γ_m, γ_t are the volume fractions of matrix and carbon nanotubes, respectively;α_t, α_m are the thermal coefficients of expansion of CNT and matrix, respectively; E the modulus of elasticity of the composite which may be approximated by

$$E = \gamma_m E_m + \gamma_t E_t \tag{18}$$

The existing experimental data as presented in Table 1 is utilized to figure out the amount of residual stress than can be developed due to thermal miss-match. The obtained thermal residual stress is applied as uniform pressure at the frictional interface of CNT and matrix perpendicular to the CNT surface so that thermal contraction phenomenon can be emulated in the model as shown on Figure 2.

2.3.2. Incorporation of vdW interaction in FE model

The van der Waals interactions between two non-bonded atoms or molecules is generally presented by the Lennard–Jones (LJ) potential$V(r)$ as follows

$$V(r) = 4\epsilon\left(\frac{\delta^{12}}{d^{12}}-\frac{\delta^{6}}{d^{6}}\right) \tag{19}$$

where δ the characteristics bond length between CNT and –CH_2- units of the polymer matrix; d is the distance between non-bonded pair of atoms or molecules; $\sqrt{2}\delta$ is the equilibrium distance between the atoms; and ϵ the bond energy that develops at the equilibrium distance.

This study uses the technique to simplify the computation by considering the number of atoms per unit surface area of CNT and number of molecules per unit volume of polymer rather considering individual atom or molecules interactions. The idea was primarily developed by Jiang et al. (2006) where they developed the normal cohesive force between matrix and graphene sheet and they further developed the formulation for MWCNTs with polymer matrix [57, 58, 59].

Table 1. Value of parameters.

Property Description	Value
Domain Size of the axisymmetric Model	10 nm × 10 nm
Diameter of CNT	1 nm
Indenter tip displacement	0.788 nm
Number of CNT in the domain	9
Bias Ratio for meshing	10
No of element in each dimension	100
Modulus of Elasticity of CNT, E_t	1000 GPa
Poisson's Ratio of CNT, ν_t	0.27
Modulus of Elasticity of Epoxy, *Em*	3000 MPa
Poisson's Ration of Epoxy, ν_m	0.35
Thickness of CNT	0.034 nm
α_t	2×10^{-6} nm/nm/°C
α_m	27.1×10^{-6} nm/nm/°C
ΔT	200°C
Coefficient of friction, μ	0.25
ϵ	0.004656 ev (1ev = 1.602×10^{-19} j)
n_p	3.1×10^{28} /m^3
n_c	3.82×10^{19} /m^2
O_i	0.2 nm

For convenience, the derived formulas and terms are recalled here briefly. CNTs as presented to the FE model of Figure 1, a 2D analytical composite model is developed to determine the interactions between CNT and polymer due to vdW interaction as shown in Figure 2. In the model, an infinite matrix is approximated where h is the equilibrium distance between CNT and matrix and O_i the average interface opening gap beyond equilibrium distance that results cohesive stress between the constituents. The cohesive stress is shown in the figure as red arrows.

The cohesive energy stored due to the van der Waals interaction in a surface area dA of CNT embedded in a polymer volume dV can be written as

$$\varphi_{dA} = n_c dA \int V(r) n_p dV \tag{20}$$

wheren_c, $n_p$are the number of atoms per unit area of nanotube and number of polymer atoms per unit volume, respectively. Using the geometry of CNT and polymer matrix, and then performing integration over the total volume of the composite, the cohesive energy due vdW interactions may be determined as follows

$$\varphi = \frac{2\pi}{3} n_c n_p \epsilon \delta^3 \left(\frac{2\delta^9}{15(h+O_i)^9} - \frac{\delta^3}{(h+O_i)^3} \right) \tag{21}$$

Now, differentiating the Eq. (21) with respect toO_i, the normal cohesive stress due to vdW interactions may be determined as follows

$$q_{vdW} = 2\pi n_p n_c \epsilon \delta^2 \left\{ \frac{1}{\left(0.4\frac{1}{\delta} + \frac{O_i}{\delta}\right)^4} - \frac{0.4}{\left(0.4\frac{1}{\delta} + \frac{O_i}{\delta}\right)^{10}} \right\} \tag{22}$$

Using Eq. (22), the normal cohesive stress due to vdW interaction between the CNT/matrix interface is presented on Figure 3 [59]. The relationship shows that the cohesive stress increases up to a peak value of 500 MPa at an interface displacement of 0.05 nm. After the peak value, cohesive stress decreases as the interface displacement increases. Previously, authors also developed an improved shear lag model for CNT based composites where transfer of radial stress is controlled by frictional interlocking, thermal miss-match coming from fabrication and more importantly the vdW interactions [60]. In the proposed study, the cohesive stress caused by vdW interaction is utilized quite similarly at the non-bonded CNT/matrix interface.

2.4. Incorporation of CNT/Matrix interface in FE model

As described earlier the CNT is frictionally interlocked with the matrix at the interface. The thickness of the CNT is kept as it is obtained from the literature and this thickness covers the physical thickness of CNT up to the equilibrium position. The theoretical interface gap between matrix and equilibrium position is filled by the matrix with the assumption that the zone strength is governed by the weak matrix strength. In another word, since the strength and stiffness of CNT is much higher than the potential matrices for nanocomposites, the properties of the interface up to the equilibrium distance are considered to be the same as the matrix material and an equivalent solid (instead of atoms) as shown in Figure 4. This radial stress which is highly sensitive with the interface displacement (as shown on Figure 3a) is accounted with the geometric nonlinearity.

In this study, thermal residual stress is assumed to be act as constant pressure along the periphery of the CNT's wall. On the other hand, vdW interaction is function of interface displacement beyond the equilibrium distance and other vdW parameters. The relative radial displacement is considered to be at the initial equilibrium distance that changes as the indenter penetrates through the nanocomposite. The relative radial displacement at the frictional interface that actually changes due to the progress of indenter tip is accounted in every step from the consideration of geometric nonlinearity as shown in Figure 5. The changes of the interface displacement also change the cohesive stress due to vdW interaction at the next step and the procedure continues till last step of the analysis. Flow chart shows how to conduct FE analysis for both perfect and non-bonded interface though this study primarily deals with non-bonded interface. All the values of the parameter are presented in Table.1.

2.5. General equations for indentation relationships

In order to obtain the mechanical properties of the nanocomposites, the results are extracted from the FE analysis which is finally processed as force displacement relationships of the indenter tip shown in Figure 6. In the analysis process, it is assumed that the area of contact between the indenter and the specimen remains constant while the unloading stage begins. The mechanical properties such as hardness and modulus of

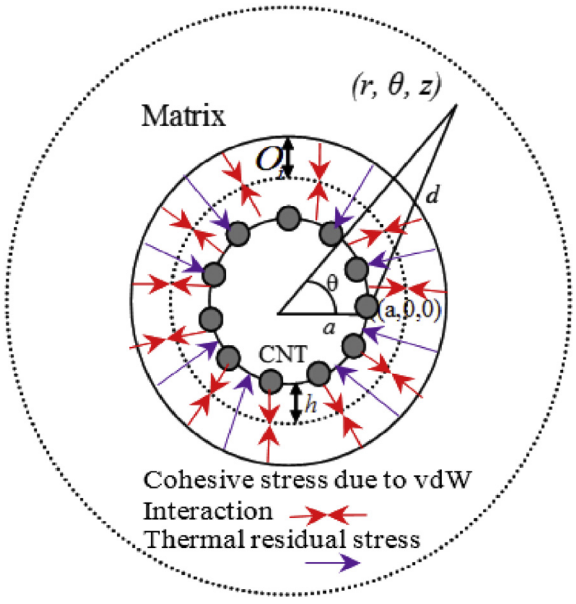

Figure 2. A 2D model showing the stresses due to vdW interaction and thermal residual stress at CNT/matrix interface.

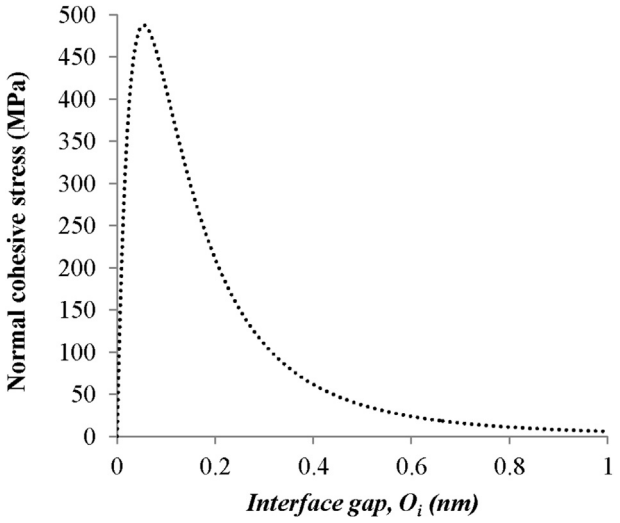

Figure 3. Normal cohesive stress due to vdW interaction with interface displacement for CNT/matrix interface.

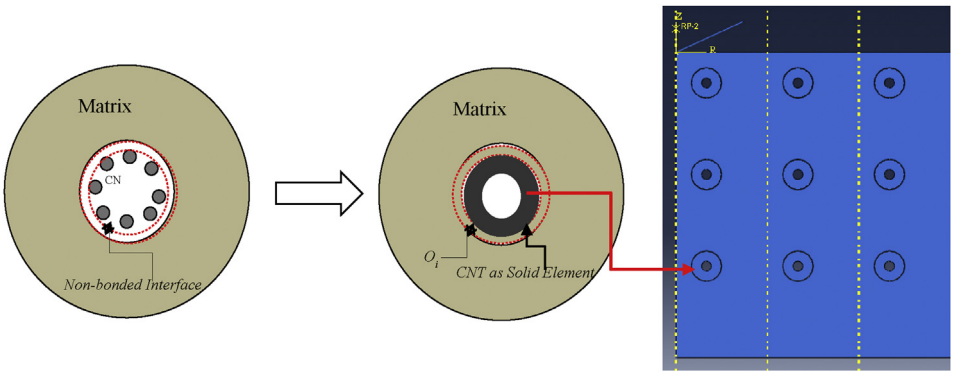

Figure 4. Conversion of non-bonded interface as equivalent solid element in FE model.

elasticity are extracted from the force-displacement relation as per well-known procedure proposed by Doerner and Nix (1986).

The slope of the force vs displacement curve during unloading of the indentation is established by the following relationship [10].

$$S = \frac{|dF|}{|dh|_{h=h_i}} = \mu E_{ef} \sqrt{A_p} \tag{23}$$

where,

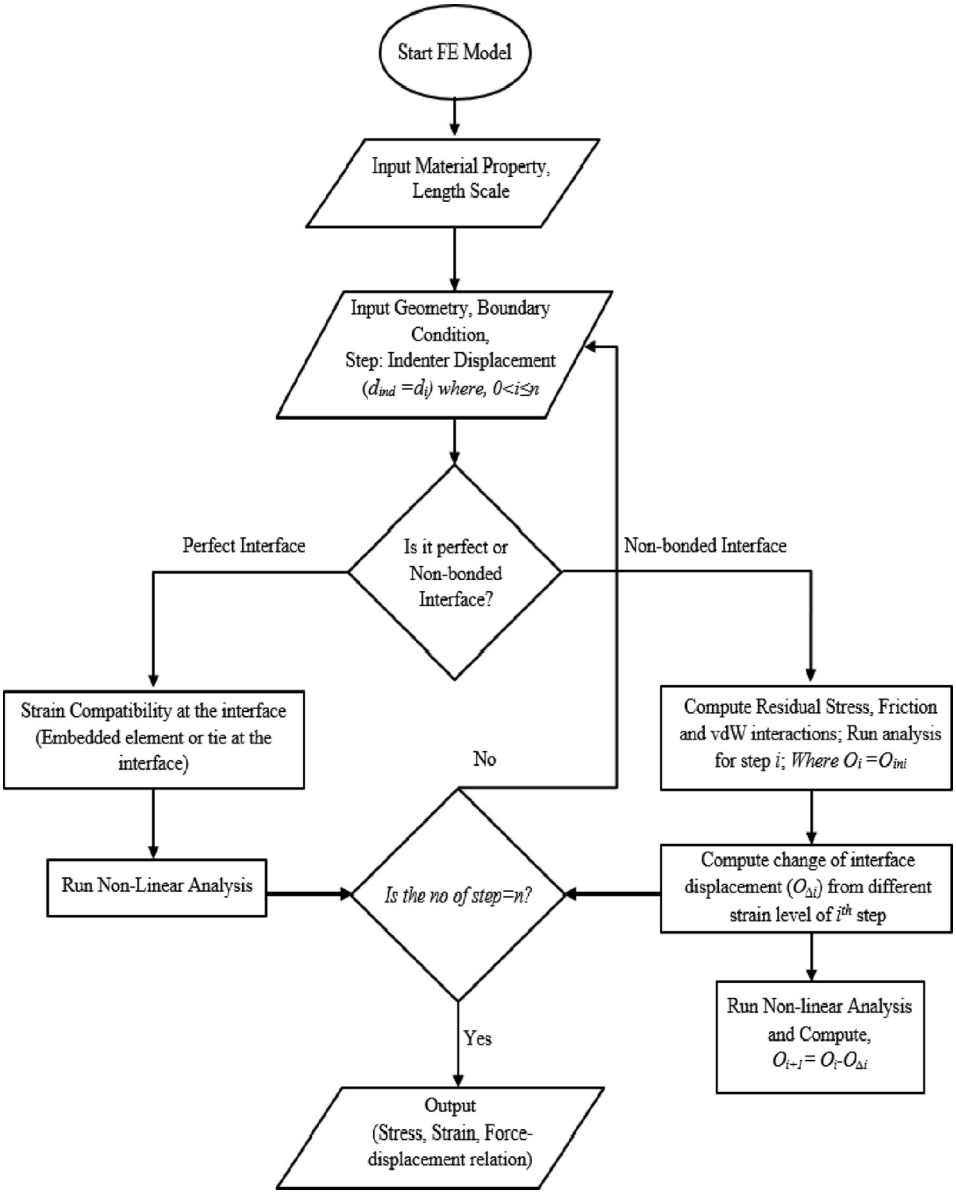

Figure 5. Flow-Chart to analyze perfect and non-bonded interface.

S the stiffness at the contact zone
h_t the total indentation depth
A_p the projected area of the contact surface
$\mu = 2\sqrt{\pi}$ value of a constant for axisymmetric indenter
$\mu = 1.167$ for Berkovich indenter

The projected area of the contact surface may be expressed as a function of indentation depth by the following equation

$$A_p = kh_p^2 \tag{24}$$

where,
h_p indentation depth
$k = 24.5$, for Berkovich &Vicker indentation

The hardness (H) of the composite may be expressed as the ratio of maximum applied load to the projected contact area for Berkovich indenter inside the nanocomposite as follows

$$H = \frac{F_{max}}{A_p} = \frac{F_{max}}{24.5h_p^2} \tag{25}$$

Using Eq. (23) and Eq. (25), the mechanical properties of nanocomposites such as modulus of elasticity and hardness can be obtained.

3. Result & discussion

Finite element models for both spherical and Berkovich indentation tests are developed to investigate different scenario of indentation simulation and numerical examples. Finite Element Modeling for indentation analysis has been studied by many researchers. However, they considered perfect CNT/matrix interface and their models does not account the hollowness of the CNTs. The hollowness effect can be a very important factor when diameter to wall thickness ratio is significantly high. To the best of author's knowledge, a combination of length scale effect and non-bonded CNT/matrix interface for nanocomposite to investigate up to a fraction of nanometer scale has never been studied. Considering all practical factors of CNTs and their potentials matrices, a series of Finite Element model has been simulated to obtain the accurate indentation output and the influences of different composite parameters. The parameters used in the finite element model are presented in Table 1.

3.1. Model validation

Before going to discuss numerical examples of indentation analysis and parametric study, the proposed model is validated with the experimental work conducted by Nouri et al. (2012) [31]. In the modeling process, Berkovich indenter having 65.3^0 indentation angle and a depth of 740 nm, mechanical properties of aluminum and MWCNT are exactly followed as per their experimental indentation test.

Nanoindentation model for 2% (by vol.) MWCNT reinforced AL-2024 nanocomposite is created and compared with that of the experimental indentation test. The stress strain relation of AL-2024 is extracted from the previous study conducted by Bastawros et al. (2006) [61]. Figure 7 shows a comparison of the force displacement relationship between numerical and experimental indentation test for 2% MWCNT reinforced AL-2024 nanocomposite. Von mises stress distribution of the nanocomposite is presented on Figure 8 (a) and stress distribution for pure Aluminium matrix is presented on Figure 8(b). The stress distribution shows that MWCNT experiences larger stress than the adjacent matrix that justify the reinforcing potential of MWCNT. It is also observed from the stress distribution that there are breaks of stress flows once they reach the MWCNTs. Therefore, the numerical result for the nanocomposite well agrees with the experimental result in both loading and unloading stage. Though the curves intersect each other in some indentation depths, they follow the same trends and similar material behavior. The minor differences between the results may arise from the considerations that the numerical model considers the uniform dispersions of CNT, the indenter as analytical rigid and perfect orientation.

However, it's nearly impossible to achieve uniform dispersion, perfect rigid indenter with infinite stiffness and theoretical orientation of a nanocomposite that is experimentally tested. The correlation obtained by numerical analysis appears indistinctly uneven in some points that actually happens due to the account of material and geometric nonlinearity as well as the vdW interactions at the non-bonded interfaces.

A further FE model is created and analysis has been run for pure AL-2024 without the presence of CNTs for verification. The obtained stress distribution due to indentation of pure aluminum matrix is presented on Figure 8b. The comparison for pure AL-2024 matrix in terms of force to indentation depth relationship between current study and the study conducted by Nouri et al. (2012) is presented on Figure 9. The comparison indicates the numerical result extracted from the proposed model agrees well with that of the experimental test. Both of the relations suggest that with as the indentation depth increases, indentation force also increases instantaneously at the loading stage. The numerical result also matches in the unloading stage except there is a difference of residual displacement at the end. This may happen due to the fact that the large strain elasto plastic model considers the length scale effect and able to capture the related effects at nano scale where the comparison is with the experiment, conducted at the micro scale.

Based on the maximum indentation depth, the values of hardness and modulus of elasticity for pure aluminum and 2% MWCNT reinforced aluminum nanocomposite are extracted from both experiments and proposed numerical analysis. The values of modulus of elasticity and

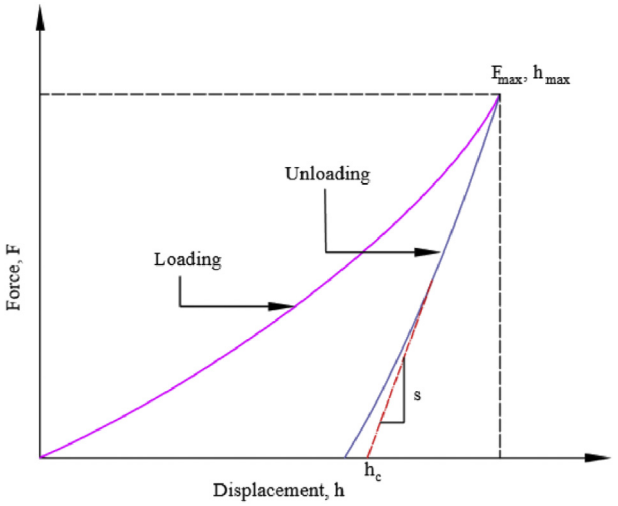

Figure 6. Schematic drawing for the determination of the material properties from indentation test [26].

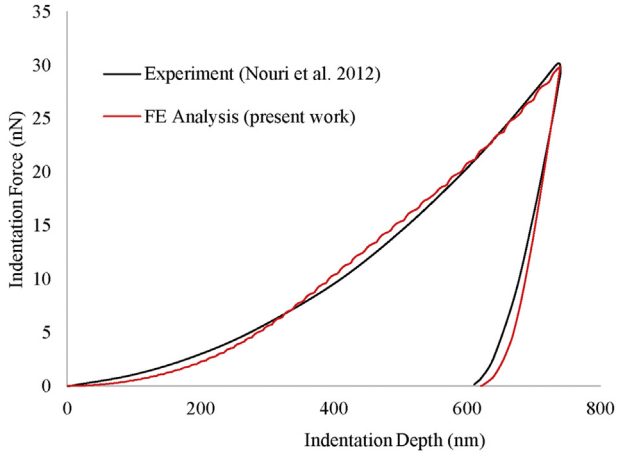

Figure 7. Comparison between present work and the experiment on 2% (by vol.) MWCNT reinforced AL-2024.

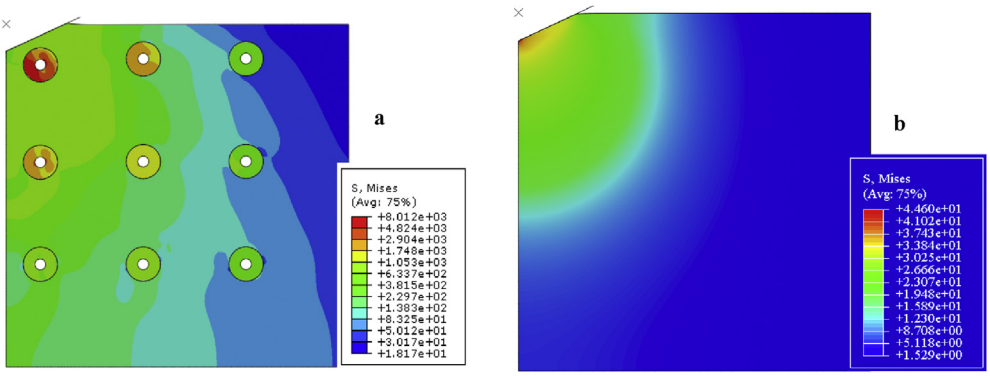

Figure 8. **(a)** Stress distribution of nanoindentation simulation of MWCNT reinforced aluminum nanocomposite; **(b)** Stress distribution of pure aluminum matrix.

Hardness of nanocomposites are extracted from the force displacement relationships using the general equations of nanoindentation as stated in Eq. (23) and Eq. (25), respectively. They are presented on Table 2. It can be clearly observed from the table that the hardness and modulus of elasticity of pure aluminum obtained from current numerical analysis are very close to that obtained from the experimental work. In case of 2% MWCNT reinforced nanocomposites, proposed numerical model shows a very good agreement with the experimental outcome. The differences of hardness and modulus of elasticity values between numerical and experimental are below ±3% and ±1%, respectively. Therefore, it can be concluded that the proposed model is able to capture the mechanical properties of nanocomposites quite accurately at nano scale.

3.2. Perfectly bonded and non-bonded CNT/matrix interface

An inclusive study is performed to investigate the influence of perfectly bonded and non-bonded CNT/matrix interface. One model is created for perfectly bonded CNT embedded in pure epoxy matrix. In order to represent perfectly bonded interface, surface to surface interaction is considered to be tie which in fact represents the strain compatibility at the interface. In another model, CNT is embedded in the epoxy matrix with non-bonded interface where stress transferring is controlled by frictional interlocking, thermal match and vdW interactions. Figure 10 shows a comparison in the form of force displacement relationship among the non-bonded interface, perfectly bonded interface and pure epoxy. All force displacement relationship indicates that indentation force increases nonlinearly as indentation progresses. In a simplified case, the result shows that the force displacement curve follows the similar trends as proposed by Harsono et al. (2009) [19]. Considering similar type of matrix, the result was further substantiated in terms of the force-displacement relationship trends that matches well with the result proposed by van Melick (2003) [8]. It can be seen from the Figure 10 that with the application of CNT, the force requirement for same indentation depth significantly increases compare to the pure epoxy polymer. It is also observed from the figure that with the addition of carbon nanotube in epoxy matrix, required indentation force increases compare to that of the pure matrix corresponding to the same displacement. As an example, the maximum required forces for 0.50 nm indentation depth are observed to be 1.53 nN and 1.32 nN for non-bonded nanocomposite and pure epoxy, respectively. The slope of the force-displacement relationship of nanocomposite is also steeper than that of the pure epoxy matrix for the cases of both loading and unloading stages. For this particular case, it is observed that with the addition of 1.3% SWCNT (by volume) in epoxy matrix, the hardness can be increased by 17% for non-bonded interface where perfect interface results a 21.5% improvement in hardness. The stress distribution of nanocomposite due to the spherical indentation is presented in Figure 11. The distribution also clearly shows that the CNT takes much larger stress than the matrix which in fact reflects the reinforcing potential of nanocomposite even for a non-bonded interface. It is understandable that highest improvement in terms of mechanical strength of a nanocomposite can be fabricated if perfect bonding is achieved at the interface. However, it is not practical to manufacture completely pure CNTs and there is always an uncertainty of uniform chemical bonding between CNT and matrix.

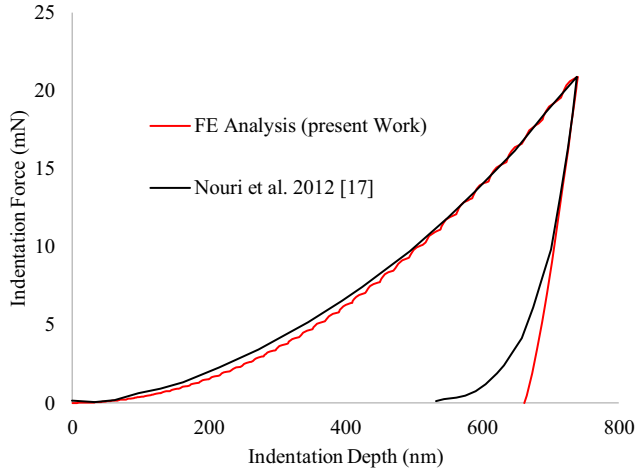

Figure 9. Comparison between present work and the study conducted by Nouri et al. (2012) on pure aluminum matrix.

3.3. Numerical examples of indentation analysis for nanocomposites

This numerical example of indentation test is performed to investigate the reinforcing potential of SWCNT and MWCNT and their suitability in polycarbide, polypropylene and aluminum (AL-2024) nanocomposite. In this part of the study, Berkovich indenter is used and non-bonded CNT/matrix interfaces for nano-composites are considered in the FE models. The mechanical properties of pure polycarbide and polypropylene are extracted from the true stress strain curve proposed by Amoedo and Lee (1992) [62]. The mechanical properties of aluminum is taken from the stress-strain curve taken from the study of Bastawros et al. (2006) [61]. The results are compared among SWCNT, MWCNT reinforced nanocomposites and pure matrix for all three cases.

Firstly, the results extracted from this study on, SWCNT and MWCNT reinforced nanocomposite and pure polycarbide are presented on Figure 12. The force indentation relationship confirms that with the presence of CNTs the force requirement increases significantly for nanocomposite compare to that of the pure polycarbide matrix. The slopes of the loading curves of nanocomposites are steeper than the pure matrix. Based on the maximum indentation force, hardness value of SWCNT and MWCNT reinforced polycarbide are 45% and 40%, respectively and both of them are higher than the pure polycarbide matrix. In

Table 2. Comparison between current study and previous experiment.

Parameter	Hardness (GPa)	Modulus of Elasticity (GPa)
Pure Aluminum Matrix [31]	1.58 GPa	74
Pure Aluminum Matrix (present work)	1.6 GPa	74.6
2% MWCNT reinforced Aluminum nanocomposite (Experiment [31])	2.263	83.3
2% MWCNT reinforced Aluminum nanocomposite (present work)	2.20	82.6

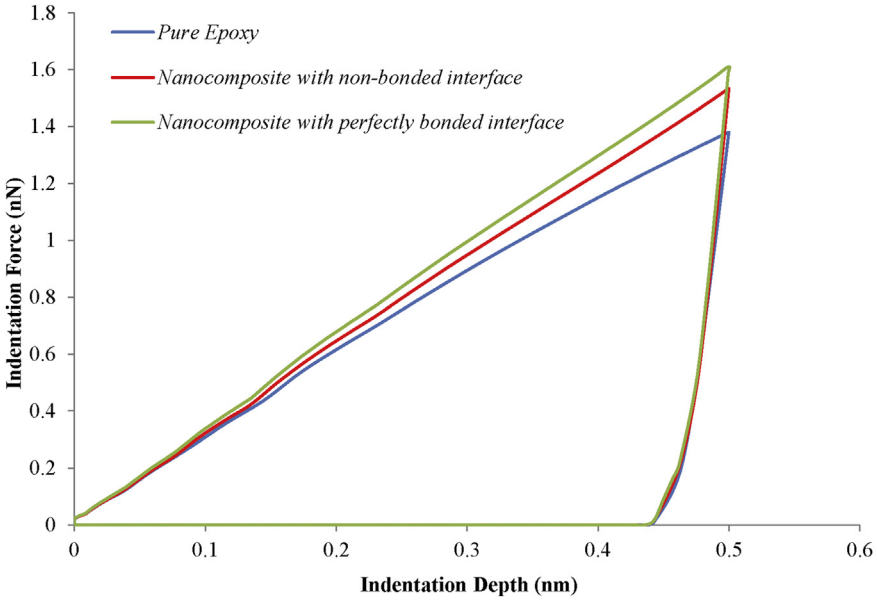

Figure 10. Force displacement relationship for perfect and non-bonded interfaces of nanocomposites.

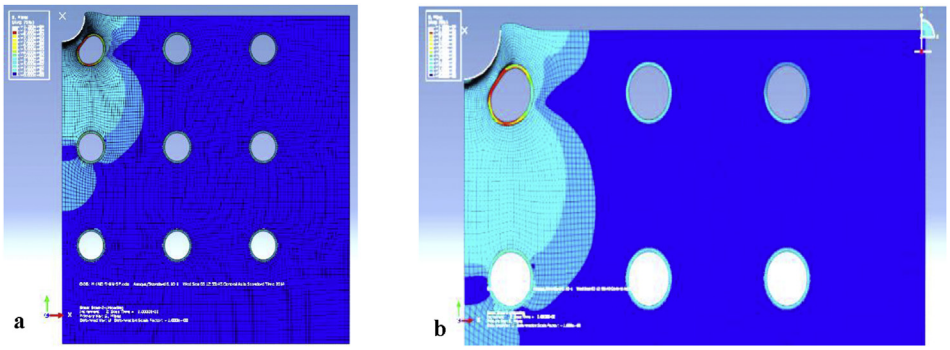

Figure 11. Stress distribution for spherical nanoindentation on SWCNT reinforced epoxy nanocomposites; (**a**) Full view of the model and (**b**) Magnified view of buckled SWCNT.

addition, the slope of the unloading stage is also much higher for SWCNT and MWCNT reinforced nanocomposite compare to that of pure polycarbide. Therefore, it can be concluded from this evidence that CNTs are significantly effective as reinforcement of polycarbide with a substantial improvement of mechanical properties of nanocomposites.

Another investigation is performed on CNT reinforced polypropylene nanocomposite. A comparison is made in terms of force displacement relation among SWCNT and MWCNT reinforced nanocomposite and pure polypropylene as presented on Figure 13. The result shows that with the presence of SWCNT or MWCNT, the indentation force increases for nanocomposite compare to that of the pure polypropylene matrix. The slopes of the loading curves of CNT based nanocomposites are significantly steeper than the pure matrix. Based on the maximum indentation force, hardness values of SWCNT and MWCNT reinforced poly carbide are 46% and 54%, respectively higher than the pure poly carbide matrix. In addition, the slope of the unloading stage is also much steeper for SWCNT and MWCNT reinforced nanocomposite compare to pure polypropylene. Therefore, it can be concluded from this evidence that CNTs are very effective as a reinforcement of polypropylene with a significant improvement of mechanical properties of nanocomposites.

Similar to the previous outcome for polycarbide, it is interesting to highlight that the slope difference at both loading and unloading stage is not much significant between SWCNT and MWCNT reinforced polypropylene nanocomposite. Based on the percentage of CNTs employed in nanocomposite and economical consideration, it can be decided that SWCNTs are more suitable and effective than MWCNTs in polymer nanocomposites such polycarbide and polypropylene nanocomposites.

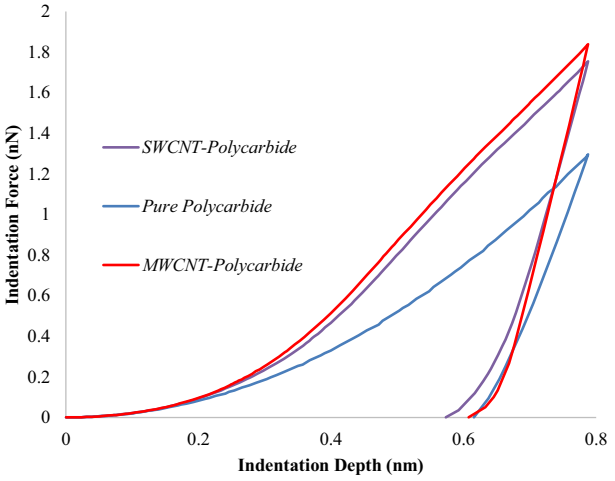

Figure 12. Force displacement relationship of SWCNT, MWCNT based polycarbide nanocomposites and pure polycarbide matrix.

The results extracted from the study on, SWCNT and MWCNT reinforced nanocomposite and pure aluminum (AL-2024) matrix are also presented on Figure 14. The result shows quite different outcome than that of the previous two numerical examples. It is clearly observed from the figure that the presence of MWCNTs results higher indentation force than pure aluminum matrix and hence improves the mechanical properties of MWCNT. However, opposite outcome is observed for SWCNT reinforced nanocomposites. It is worthwhile to mention that the slope of the loading curve of SWCNT reinforced nanocomposite is even smaller than the pure aluminum. The outcome indicates that the addition of SWCNTs does not improve the mechanical properties of aluminum reinforced nanocomposite rather it decreases the hardness and elastic values compare to the pure aluminum matrix. Based on the maximum indentation force, though presence of MWCNT in Al-2024 matrix improves the hardness value by 20.5 %, the addition of SWCNTs in same matrix reduce the hardness value as large as 40%. It is also observed from the figure that compare to others, the slope of SWCNT based aluminum composite is comparatively mild at unloading stage. This mild slope ultimately results a smaller value of modulus of elasticity for SWCNT reinforced nanocomposites compare to that of pure aluminum matrix and MWCNT reinforced nanocomposites. This important outcome may be described by the fact that the SWCNT in aluminum matrix starts buckling at the loading stage because of their high thickness to diameter ratio (D/t). The simulated buckling phenomena of SWCNT in nanocomposite with the stress distribution is presented on Figure 15. The local buckling of SWCNT reduce the force requirement compare to that of the pure aluminum matrix and hence reduced values of hardness and mechanical strength are found. However, no buckling is observed in MWCNTs and the slopes of the loading curves of MWCNT reinforce aluminum nanocomposites are significantly steeper than the pure matrix. Therefore, it is established from these evidences that MWCNTs are effective as reinforcement of aluminum with a significant improvement of mechanical properties of nanocomposites though SWCNT reduces the mechanical properties rather any improvement.

3.4. Wall thickness dependency of nanocomposites

In this part of the study, Berkovich indentation analysis is performed on CNT reinforced conventional steel nanocomposites. Analysis has been run for ten different wall thicknesses of CNTs keeping the same outer diameter. Elasto-plastic behavior of steel and CNT including strain gradient is considered in the program. Investigations are conducted in a wide range of wall thickness starting from 0.034nm to 0.334nm. The stress distribution of nanoindentation simulation for typical thin and thick walled CNTs are presented on Figure 16. The Berkovich simulation result shows that the higher stress is developed near the indenter tip. In addition, maximum von mises stress is observed in the CNTs compare to the adjacent matrix region. The stress distribution evidently shows that thin wall CNTs near the indenter are collapsed due to buckling inside the matrix. In contrast, thick wall CNT (having a diameter over 0.2 nm) seems to float inside the matrix without showing any buckling as indentation progresses. It is interesting to note that, though the indenter tip moves downward inside the matrix, the shape of the thick-walled tube remains unchanged. It is also observed from the stress distribution suggests that the stress flow is higher in lateral direction than that in vertical path.

Wall thickness dependency of CNT reinforced nanocomposites is presented in terms of force-displacement relationship as shown in Figure 17. It can be clearly understood from the figure that force requirement increases as the indenter tip progresses through the nanocomposites. However, the required force sharply increases for thicker nanotubes reinforced composites particularly after an indentation depth of 0.30nm. On the other hand, the force increment of thinner walled (0.034nm) CNT-Steel composite is not linear with the indentation depth. The difference of force requirement for same indentation depth between thin and thick walled nanocomposite is very much significant. The maximum required force of thick walled CNT-steel composite for an indentation depth 0.788nm is nearly 2.5 times than that of the thinnest CNT-Steel nanocomposites. It is interesting to highlight that there is a

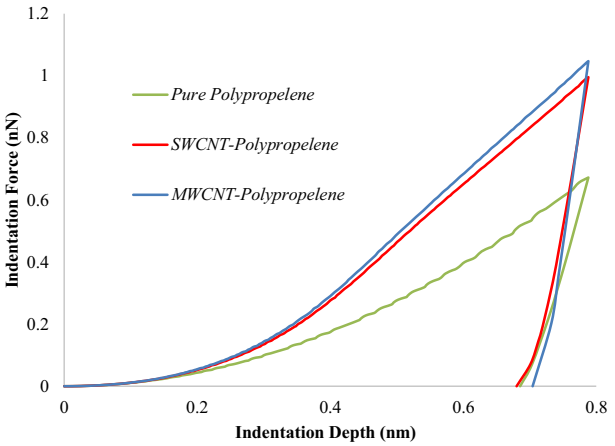

Figure 13. Force displacement relationship of SWCNT, MWCNT based polypropylene nanocomposites and pure polypropylene matrix.

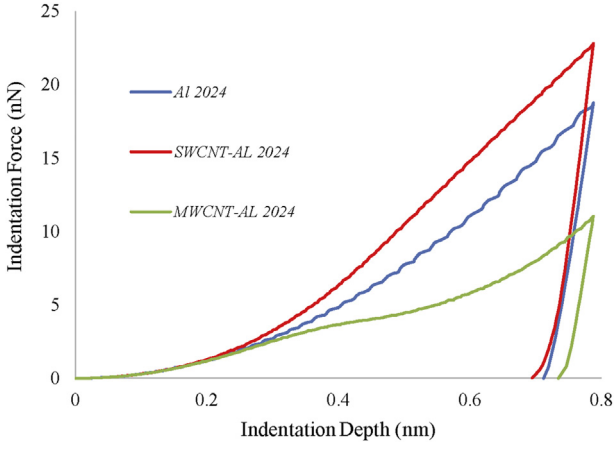

Figure 14. Force displacement relationship of SWCNT, MWCNT based aluminum nanocomposites and pure aluminum matrix.

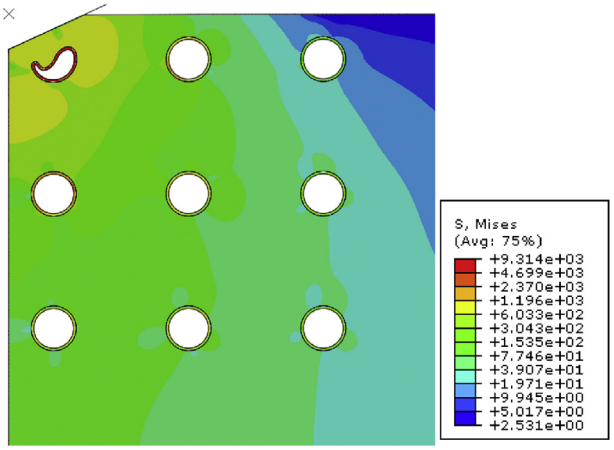

Figure 15. Stress distribution of SWCNT reinforced AL-2024 nanocomposite.

turn at the force-displacement profile for an indentation depth in the range of 0.4–0.6nm up to a wall thickness of 0.1nm. This may happen due to the fact that buckling occurs for thin wall carbon nanotubes as presented on Figure 16. This phenomenon can be explained by the fact that smaller wall thickness results local bucking of the CNTs, loses its stability and hence the resistance from the tube is insignificant in this region. However, the force requirement increases sharply after an indentation depth of more than 0.6 nm. This happens because though, the CNT loses its lateral stability after initial buckling, it regains stability after further buckling as they are confined by matrix materials and show high ductile behavior inside the matrix. Similar occurrence is observed when the indentation analysis is conducted for SWCNT-aluminum nanocomposites as presented on Figure 15. It is to be noted that if wall thickness is more than 0.2nm, all CNTs having similar outer diameter give almost same indentation profile. This can be explained by the fact that lateral buckling of CNT for that particular diameter can be resisted by a wall thickness of 0.2 (diameter to thickness ratio 5.0) or higher and this wall thickness may be considered as the optimum thickness to achieve maximum influence of CNT in nanocomposites for a fixed outer diameter of 1nm.

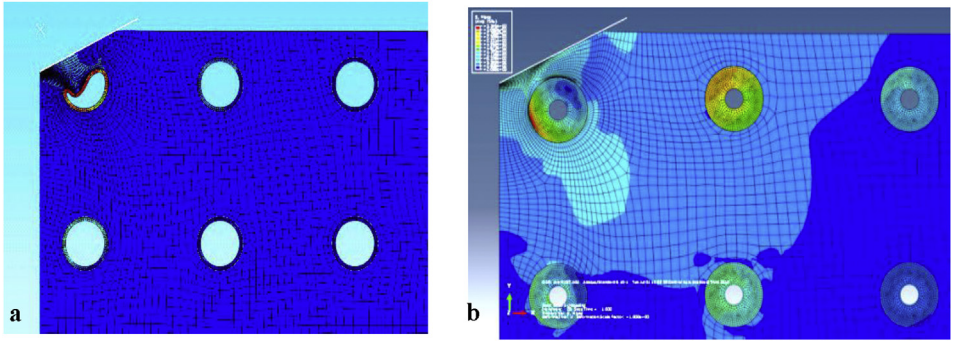

Figure 16. Stress distribution of Berkovich nanoindentation simulation for **(a)** thin-walled and **(b)** thick-walled nanotube reinforced composites.

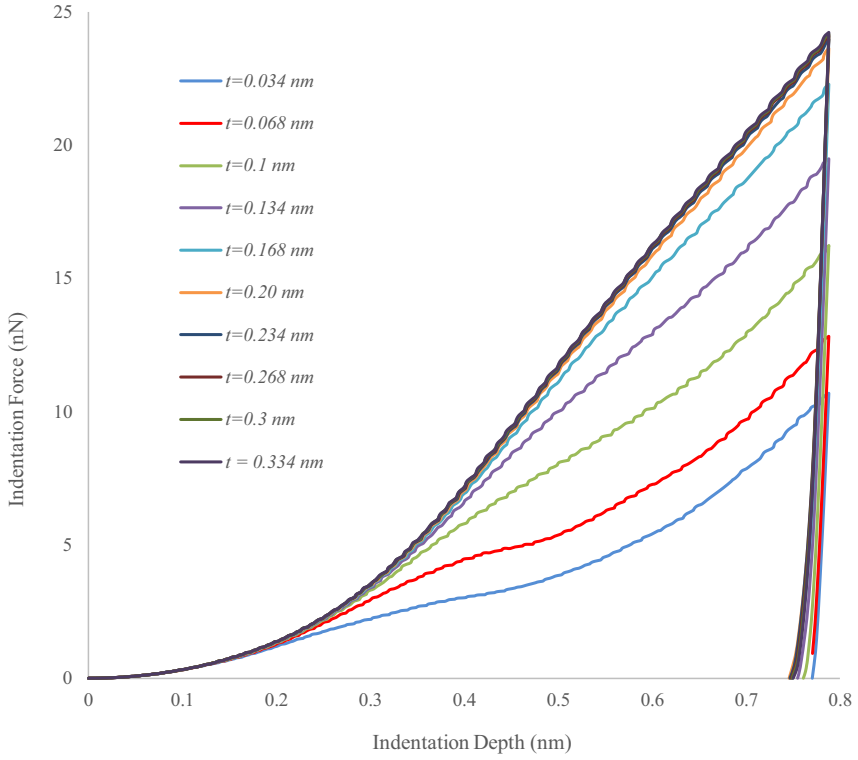

Figure 17. Force displacement relationship for different wall thicknesses of CNTs in nanocomposites.

Figure 18 shows the variation of modulus of Elasticity of nanocomposites (E_{nc}) with the wall thickness of CNTs. The values of modulus of elasticity of nanocomposite are extracted from the force displacement relationships of wall thickness dependency study. The result shows that with the increase of wall thickness of CNT, modulus of elasticity of the composite also increases though the increment does not change linearly. Initially, the variation of E_{nc} with respect to wall thickness is much steeper than that of the wall thickness greater than 0.2 nm. It is very worthwhile to mention that the modulus elasticity of CNT-steel nanocomposite for a wall thickness of less than 0.05nm (SWCNT) is observed to be nearly 180 GPa which is less than that of pure steel (Es = 200 GPa). Therefore, SWCNTs are found to be ineffective as a reinforcement of pure steel matrix. This behavior is similarly observed for SWCNT reinforced aluminum nanocomposites as presented on Figure 14.

Figure 19 presents the wall thickness dependency of hardness of CNT reinforced nanocomposites. It is also observed from the figure that hardness sharply increases with the increase up to a wall thickness of 0.2 nm and it remains nearly constant after that value. This hardness behavior of nanocomposite can be described as, large distortion of CNT occurs for smaller wall thickness of CNTs. In addition, bond strength between collapsed CNT and adjacent matrix become weaker because cohesive stress due to vdW interactions becomes insignificant as the interface goes far away from the equilibrium distance. Therefore, in order to achieve a desired hardness for nanocomposite, this study may provide a preliminary guideline to design the optimum wall thickness for particular matrix so that CNTs can effectively contribute to the composite properties.

3.5. Influence of CNTs positioning on material properties of nanocomposites

A separate study is also performed to investigate the influences of CNTs positioning inside the matrix on the material properties of nanocomposites. Based on the study conducted on CNT reinforced steel nanocomposites, a total five indenter's position was examined. Force displacement relationship of the numerical analysis for different indenter positions is presented on Figure 20. It can be seen from the figure that force requirement increases with the decrease of nanotube's distance from the indenter tip for a particular indentation depth greater than 0.2 nm. It is also understood that the force displacement relationship is observed to be nonlinear and there is clear unevenness on the curves. Such behavior may happen due to the account of geometric nonlinearity with the abrupt variation of vdW interaction at the CNT/matrix interface of nanocomposite. In addition, it is clearly observed from the figure that the presence of CNTs in nanocomposite influences the relationship significantly compared to that for pure steel. It is also exciting to note that CNTs position closer than 0.5nm from the indenter provides similar force displacement relationship. Such study may help in designing future nanostructures where individual CNTs positing can be monitored and fixed as per requirement.

3.6. Influence of volume fraction of CNTs

In this part of the study, influences of volume fraction on the mechanical properties of metal matrix nanocomposites are investigated using Berkovich nanoindentation. In the comparison, SWCNT, double walled CNT (DWCNT) and multi walled CNTs (MWCNT) are taken into consideration. Volume fraction is calculated from the theoretical volume of CNTs to the total volume of the composite. Theoretical volume of CNTs is calculated here from the sum total of the volume of each nanotube (after reducing the volume due to hollowness of CNTs) multiplied by the number of tube where different tube cross section with different numbers are employed.

The influence of volume fraction of CNTs on nanocomposite is presented on Figure 21. As can be seen from the figure that maximum indentation force requirement for 1.6% DWCNT or 2.5% MWCNT are more than double of that for 1.3% SWCNT. As sated earlier, this may happen due to the fact that SWCNT experiences local buckling under small indentation depth. Subsequently, mechanical properties such as hardness and modulus of elasticity of nanocomposites are much higher

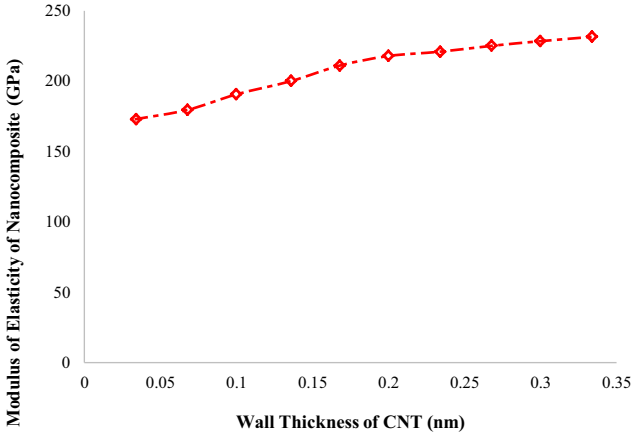

Figure 18. Influence of CNT's wall thickness on the modulus of elasticity of nanocomposites.

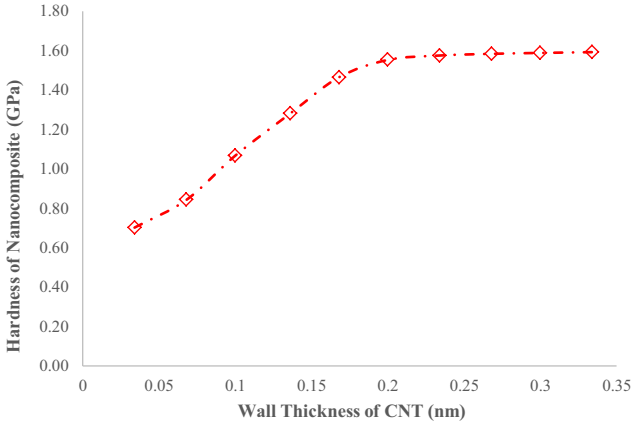

Figure 19. Influence of CNT's wall thickness on the hardness of nanocomposites.

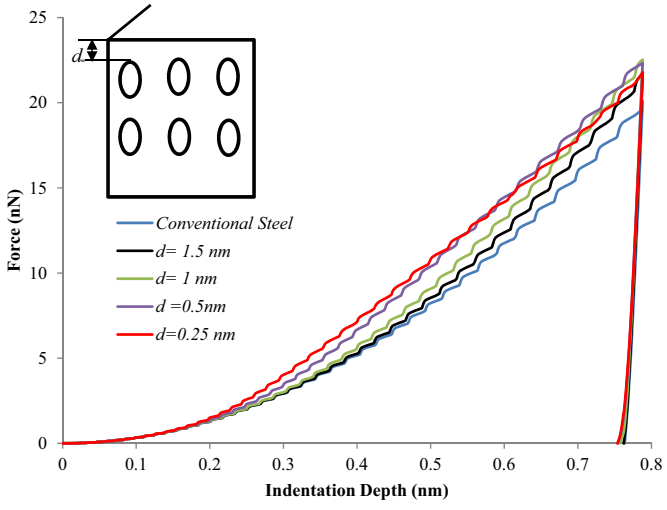

Figure 20. Force displacement relationship for different CNTs positioning in nanocomposites.

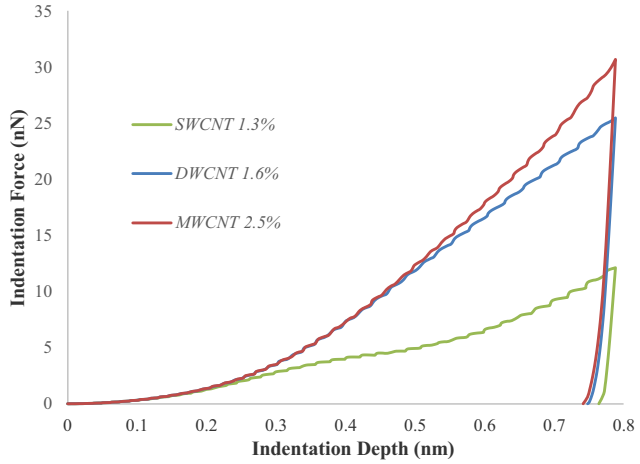

Figure 21. Force displacement of different volume fractions of CNTs in nanocomposites.

for DWCNT or MWCNT than that of the SWCNT, even though the difference of volume fraction is not much higher. In addition, the residual indentation depth is significantly higher for SWCNT than that of DWCNT and MWCNT. Therefore, it can be concluded from this result that volume fraction of CNT is not the only criteria to improve the mechanical properties of CNT reinforced composites but also the number of CNT types significantly influences the nanocomposite. It is to be noted that the study on volume fraction is conducted on metal matrix nanocomposites and different behavior may be observed if it is conducted on polymer nanocomposites. Based on this study, optimum volume fraction of CNTs for a particular nanocomposite may be suggested by a combined investigation on the type of matrix, types of CNTs and their wall thickness.

3.7. Influence of strain hardening parameter (n)

In this part of the study, influence of strain hardening parameter of matrix on the SWCNT based nanocomposite properties are investigated. Force indentation relationship for four different strain hardening parameters of matrices is presented on Figure 22. It can be seen from the figure that, with the increase of the value of strain hardening parameter (n), force requirement decreases accordingly for the same penetration of the indenter in nanocomposites. In addition, it is also observed from the

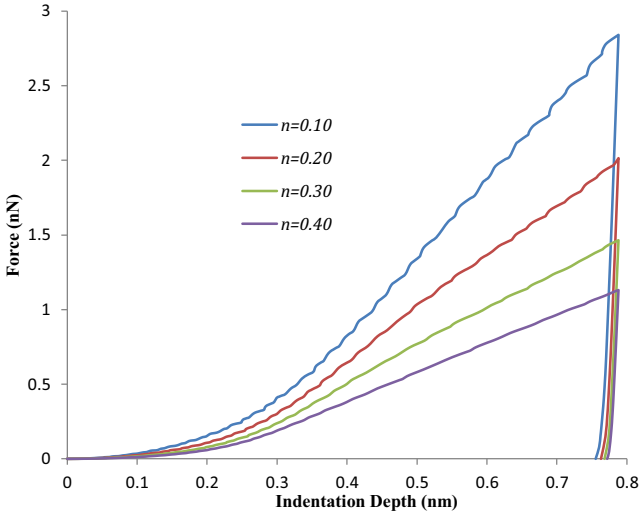

Figure 22. Force displacement relationship of nanocomposite for different values of strain hardening parameter of matrix.

figure that with the increase of the value of *n*, residual indentation displacement decreases accordingly. This can be explained by the fact that with the increase of the value of *n*, plastic strain also increases for same stresses of the matrix. It is also observed from the figure that, the deviation of forces is higher if the value of *n* is close to 0.1. For example, the difference between maximum indentation forces, (F_{max}) between n values of 0.1 and 0.2 is more than double of that difference of F_{max} between *n* values of 0.3 and 0.4. Therefore, it can be concluded from the result that the relationship and hence the properties of nanocomposites are largely dependent on the hardening parameter. Based on this result, it may be suggested that matrices having strain hardening parameter near to the value of 0.1 may enhance composites properties more effectively by the addition of this particular type of CNTs.

4. Conclusion

A number of finite element models have been developed to investigate indentation analysis for uniformly dispersed CNTs in different matrices in which non-bonded CNT/matrix interface and large strain elasto-plastic behavior of constituents are considered. The proposed finite element model for nanoindentation analysis is validated with the experimental indentation test on 2% (by vol.) MWCNT reinforced aluminum nanocomposites conducted by Nouri et al. (2012) [31]. The comparison shows that the proposed technique demonstrates a very good agreement with their experimental result. The differences of modulus of elasticity and hardness between experimental indentation test and this advanced finite element simulation are below 1% and 3%, respectively.

The study on the influence of chemically bonded and non-bonded interface shows that the mechanical properties of CNT reinforced polymer composites significantly improves for both bonded and non-bonded CNT/matrix interfaces. It is observed from the spherical indentation simulation that with the addition of 1.3% SWCNT in epoxy resin can improve the nanocomposite by 17% in terms of hardness for non-bonded interface which is only 3.5% less than that for perfectly bonded interface. This outcome noticeably highlights that the bonding condition plays a significant role in determining composite properties. This difference may depends on other material parameters and types of CNTs, their proportions and potential matrix properties. This study also suggests that if perfect bonding at the interface is not achieved in a nanocomposite, they should be idealized and accounted as non-bonded interface so that overestimation of composite parameters can be avoided and accurate material properties of nanocomposites is obtained.

Numerical examples of nanoindentation analysis on different matrices shows very interesting outcome. The results are presented for SWCNT, MWCNT reinforced polycarbide, polypropylene and aluminum nanocomposites along with their pure matrices. The result concludes that SWCNT are very effective in polymer composites like polycarbide and polypropylene. However, SWCNTs are less efficient in metal matrix nanocomposites such as SWCNT reinforced aluminum or steel nanocomposites. In some cases, they may even reduce the strength of nanocomposites because local buckling occurs in SWCNTs before reaching their mechanical yield strength. On the other hand, MWCNTs are very efficient for all types of matrices and significantly improve the mechanical properties of nanocomposites. This study suggests SWCNTs to be used as reinforcement for polymer composites and MWCNTs as reinforcement for all type composites more particularly for metal matrix nanocomposites.

The study on wall thickness dependencies of CNTs in nanocomposite shows that mechanical properties of nanocomposites largely depends on the wall thickness of CNTs. A minimum wall thickness for a particular tube diameter to achieve a pick value of hardness and modulus of elasticity of nanocomposites is determined. The minimum wall thickness of CNTs is suggested to be 0.2nm for an outer diameter of 1nm in order to achieve the maximum value composite properties. In addition, a wall thickness smaller than 0.05nm may even reduce the hardness and modulus of elasticity of CNT reinforced composites compare to that of

pure matrix. This happens due to the fact that large distortion occurs for smaller thickness. In addition, this distortion of CNTs changes the relative radial displacement at the CNT/matrix interface causing a smaller stress transfer through the interface and hence results smaller values of hardness and modulus of elasticity of nanocomposites.

An investigation on nanotube's relative positioning with the indenter tip is conducted to obtain its influence on the composite parameter. For a particular types of CNTs, mechanical properties of nanocomposites significantly improves as CNTs come closer to indenter. However, the improvement stops once CNT is close to 0.5 nm from the indenter tip. The parametric study on the changes of volume fraction of CNTs reveals that composite parameters significantly depends on the number of walls like DWCNT or MWCNT rather than the theoretical volume fraction of CNTs alone. The study on the variation of strain hardening parameter shows that the performance of nanocomposites largely depends on the value of strain hardening parameters of matrix. This study suggests the value of strain hardening parameter of matrices to be close to 0.10 that can efficiently improve the mechanical properties for CNT reinforced nanocomposites.

One of the major achievements of this study is to develop a new technique of indentation simulation that can capture both length scale effect and the controlling factors for non-bonded interface such as mechanical interlocking, thermal residual stress and van der Waals interactions. Previous research on nanoindentation may come with a convenient solution for carbon nanotube reinforced composites for the chemically bonded i.e. perfectly bonded CNT/Matrix interface. However, this study is a noble solution for non-bonded interface where size effect and non-bonded CNT/matrix interfaces are incorporated in Finite element simulation rather a perfect interface. Furthermore, parametric studies on wall thickness dependency, influences of nanotubes positioning and straining hardening parameter of the matrix are also new contribution for CNT reinforced nanocomposites. Therefore, this study may contribute in designing different type of carbon nanotube reinforced nanocomposites and their appropriate application as reinforcement of different nanostructures.

Declarations

Author contribution statement

Khondaker S. Ahmed: Conceived and designed the experiments; Analyzed and interpreted the data; Contributed reagents, materials, analysis tools or data; Wrote the paper.

Ibriju Ibrahim: Analyzed and interpreted the data; Contributed reagents, materials, analysis tools or data.

Ang K. Keng: Analyzed and interpreted the data; Wrote the paper.

Funding statement

This research did not receive any specific grant from funding agencies in the public, commercial, or not-for-profit sectors.

Competing interest statement

The authors declare no conflict of interest.

Additional information

No additional information is available for this paper.

References

[1] P.M. Ajayan, et al., Single-walled carbon nanotube–polymer composites: strength and weakness, Adv. Mater. 12 (10) (2000) 750–753.
[2] B. Ashrafi, P. Hubert, Modeling the elastic properties of carbon nanotube array/polymer composites, Compos. Sci. Technol. 66 (3-4) (2006) 387–396.
[3] S.R. Bakshi, D. Lahiri, A. Agarwal, Carbon nanotube reinforced metal matrix composites - a review, Int. Mater. Rev. 55 (1) (2010) 41–64.
[4] X. Chen, Square representative volume elements for evaluating the effective material properties of carbon nanotube-based composites, Comput. Mater. Sci. 29 (1) (2004) 1–11.
[5] X.H. Chen, et al., Dry friction and wear characteristics of nickel/carbon nanotube electroless composite deposits, Tribol. Int. 39 (1) (2006) 22–28.
[6] M.P. Manoharan, et al., The interfacial strength of carbon nanofiber epoxy composite using single fiber pullout experiments, Nanotechnology 20 (29) (2009) 295701.
[7] K.S. Ahmed, A.K. Keng, Interface characteristics of nanorope reinforced polymer composites, Comput. Mech. 52 (3) (2013) 571–585.
[8] K.S. Ahmed, A.K. Keng, Interface characteristics of carbon nanotube reinforced polymer composites using an advanced pull-out model, Comput. Mech. 53 (2) (2014) 297–308.
[9] H.G.H. van Melick, et al., A micro-indentation method for probing the craze-initiation stress in glassy polymers, Polymer 44 (8) (2003) 2481–2491.
[10] L. De Fazio, et al., Nanoindentation of CVD diamond: comparison of an FE model with analytical and experimental data, Diam. Relat. Mater. 10 (3) (2001) 765–769.
[11] Y. Kusano, I.M. Hutchings, Analysis of nano-indentation measurements on carbon nitride films, Surf. Coating. Technol. 169–170 (2003) 739–742.
[12] P.L. Larsson, et al., Analysis of Berkovich indentation, Int. J. Solid Struct. 33 (2) (1996) 221–248.
[13] J. Gou, et al., Computational analysis of effect of single-walled carbon nanotube rope on molecular interaction and load transfer of nanocomposites, Compos. B Eng. 36 (6-7) (2005) 524–533.
[14] S.J.V. Frankland, V.M. Harik, Analysis of carbon nanotube pull-out from a polymer matrix, Surf. Sci. 525 (2003) L103–L108. Chimica.
[15] V. Lordi, Y. Nan, Molecular mechanics of binding in carbon-nanotube-polymer composites, J. Mater. Res. 15 (2000) 2770–2779. Copyright 2001, IEE.
[16] M. Wong, et al., Physical interactions at carbon nanotube-polymer interface, Polymer 44 (25) (2003) 7757–7764.
[17] D. Qian, Load transfer mechanism in carbon nanotube ropes, Compos. Sci. Technol. 63 (11) (2003) 1561–1569.
[18] N. Vu-Bac, P.M.A. Areias, T. Rabczuk, A multiscale multisurface constitutive model for the thermo-plastic behavior of polyethylene, Polymer 105 (2016) 327–338.
[19] M. Haghgoo, R. Ansari, M.K. Hassanzadeh-Aghdam, Effective elastoplastic properties of carbon nanotube-reinforced aluminum nanocomposites considering the residual stresses, J. Alloys Compd. 752 (2018) 476–488.
[20] M.K. Hassanzadeh-Aghdam, R. Ansari, A. Darvizeh, Micromechanical analysis of carbon nanotube-coated fiber-reinforced hybrid composites, Int. J. Eng. Sci. 130 (2018) 215–229.
[21] M. Hassanzadeh-Aghdam, M. Mahmoodi, R. Ansari, Micromechanical characterizing the effective elastic properties of general randomly distributed CNT–reinforced polymer nanocomposites, Probabilist. Eng. Mech. 53 (2018) 39–51.
[22] K.S. Ahmed, A.K.J.W.J.o.N.S. Keng, and Engineering, Static Crack Propagation of Carbon Nanotube through Non-bonded Interface of Nanocomposites 2014 (2014).
[23] M. Haghgoo, et al., Analytical formulation for electrical conductivity and percolation threshold of epoxy multiscale nanocomposites reinforced with chopped carbon fibers and wavy carbon nanotubes considering tunneling resistivity, Compos. Appl. Sci. Manuf. 126 (2019) 105616.
[24] M.K. Hassanzadeh-Aghdam, et al., Effects of adding CNTs on the thermo-mechanical characteristics of hybrid titanium nanocomposites, Mech. Mater. 131 (2019) 121–135.
[25] M.K. Hassanzadeh-Aghdam, M.J. Mahmoodi, R. Ansari, Creep performance of CNT polymer nanocomposites-An emphasis on viscoelastic interphase and CNT agglomeration, Compos. B Eng. 168 (2019) 274–281.
[26] M.F. Doerner, W.D. Nix, A Method for Interpreting the Data from Depth-Sensing Indentation Instruments 1 (1986) 601–609.
[27] B.J. Briscoe, L. Fiori, E. Pelillo, Nano-indentation of polymeric surfaces, J. Phys. D Appl. Phys. 31 (19) (1998) 2395.
[28] H. Lee, et al., Characterization of carbon nanotube/nanofiber-reinforced polymer composites using an instrumented indentation technique, Compos. B Eng. 38 (1) (2007) 58–65.
[29] M. Cadek, et al., Morphological and mechanical properties of carbon-nanotube-reinforced semicrystalline and amorphous polymer composites, Appl. Phys. Lett. 81 (27) (2002) 5123–5125.
[30] S.I. Cha, et al., Strengthening and toughening of carbon nanotube reinforced alumina nanocomposite fabricated by molecular level mixing process, Scripta Mater. 53 (7) (2005) 793–797.
[31] N. Nouri, et al., Fabrication and mechanical property prediction of carbon nanotube reinforced Aluminum nanocomposites, Mater. Des. 34 (2012) 1–14.
[32] J. Babu, A. Srinivasan, C. Kang, Nano and macromechanical properties of aluminium (A356) based hybrid composites reinforced with multiwall carbon nanotubes/alumina fiber, J. Compos. Mater. 51 (11) (2017) 1631–1642.
[33] P. Nikaeen, D. Depan, A. Khattab, Surface mechanical characterization of carbon nanofiber reinforced low-density polyethylene by nanoindentation and comparison with bulk properties, Nanomaterials (Basel, Switzerland) 9 (10) (2019) 1357.
[34] D. Barun, et al., Nano-indentation studies on polymer matrix composites reinforced by few-layer graphene, Nanotechnology 20 (12) (2009) 125705.
[35] Q. Zhang, et al., Microstructure and nanoindentation behavior of Cu composites reinforced with graphene nanoplatelets by electroless co-deposition technique, Sci. Rep. 7 (1) (2017) 1338.
[36] J. Jyoti, et al., Synergetic effect of graphene oxide-carbon nanotube on nanomechanical properties of acrylonitrile butadiene styrene nanocomposites, Mater. Res. Express 5 (4) (2018), 045608.

[37] T. Batakliev, et al., Nanoindentation analysis of 3D printed poly(lactic acid)-based composites reinforced with graphene and multiwall carbon nanotubes, J. Appl. Polym. Sci. 136 (13) (2019) 47260.
[38] E. Harsono, S. Swaddiwudhipong, Z.S. Liu, Material characterization based on simulated spherical-Berkovich indentation tests, Scripta Mater. 60 (11) (2009) 972–975.
[39] O. Borrero-López, et al., Reverse size effect in the fracture strength of brittle thin films, Scripta Mater. 60 (11) (2009) 937–940.
[40] W. Wang, et al., Effective reinforcement in carbon nanotube-polymer composites, Phil. Trans. Math. Phys. Eng. Sci. 366 (1870) (2008) 1613–1626.
[41] A. Salehikhojin, N. Jalili, A comprehensive model for load transfer in nanotube reinforced piezoelectric polymeric composites subjected to electro-thermo-mechanical loadings, Compos. B Eng. 39 (6) (2008) 986–998.
[42] D. Qian, et al., Load transfer and deformation mechanisms in carbon nanotube-polystyrene composites, Appl. Phys. Lett. 76 (20) (2000) 2868–2870.
[43] K. Liao, S. Li, Interfacial characteristics of a carbon nanotube–polystyrene composite system, Appl. Phys. Lett. 79 (25) (2001) 4225.
[44] M.P. Manoharan, et al., The interfacial strength of carbon nanofiber epoxy composite using single fiber pullout experiments, Nanotechnology 20 (2009) 295701. Copyright 2009, The Institution of Engineering and Technology.
[45] L. Kin, L. Sean, Interfacial characteristics of a carbon nanotube-polystyrene composite system, Appl. Phys. Lett. 79 (2001) 4225–4227. Copyright 2002, IEE.
[46] K.S. Ahmed, K.K. Ang, and Structures, A pull-out model for perfectly bonded carbon nanotube IN polymer composites 7 (2012) 753–764.
[47] M.A. Msekh, et al., Fracture properties prediction of clay/epoxy nanocomposites with interphase zones using a phase field model, Eng. Fract. Mech. 188 (2018) 287–299.
[48] H. Talebi, et al., A computational library for multiscale modeling of material failure, Comput. Mech. 53 (5) (2014) 1047–1071.
[49] L. Minh-Tai, S.-C. Huang, Mechanical characterization of carbon nanotube-reinforced polymer nanocomposite by nanoindentation using finite element method, Sensor. Mater. 27 (8) (2015) 617–624.
[50] G.I. Taylor, The mechanism of plastic deformation of crystals. Part I.—Theoretical, Proc. Roy. Soc. Lond. Ser. A 145 (855) (1934) 362–387.
[51] K.N. Solanki, et al., Magnesium Technology 2017, Springer, 2017.
[52] W.C. Ashby, Physics and chemistry of the atmosphere, Ecology 55 (4) (1974), 916-916.
[53] S. Li, X.-L. Gao, Handbook of Micromechanics and Nanomechanics, Jenny Stanford Publishing, 2016.
[54] S. Kok, A.J. Beaudoin, D.A. Tortorelli, A polycrystal plasticity model based on the mechanical threshold, Int. J. Plast. 18 (5) (2002) 715–741.
[55] J.M. Wernik, S.A. Meguid, Atomistic-based continuum modeling of the nonlinear behavior of carbon nanotubes, Acta Mech. 212 (1) (2010) 167–179.
[56] B. Budiansky, J.W. Hutchinson, A.G. Evans, Matrix fracture in fiber-reinforced ceramics, J. Mech. Phys. Solid. 34 (2) (1986) 167–189.
[57] L.Y. Jiang, A cohesive law for carbon nanotube/polymer interface accounting for chemical covalent bonds, Math. Mech. Solid 15 (7) (2010) 718–732.
[58] Y. Jiang, et al., Measurement of radial deformation of single-wall carbon nanotubes induced by intertube van der Waals forces, Phys. Rev. B 77 (15) (2008).
[59] L.Y. Jiang, et al., A cohesive law for carbon nanotube/polymer interfaces based on the van der Waals force, J. Mech. Phys. Solid. 54 (11) (2006) 2436–2452.
[60] K.K. Ang, K.S. Ahmed, An improved shear-lag model for carbon nanotube reinforced polymer composites, Compos. B Eng. 50 (2013) 7–14.
[61] A.F. Bastawros, Analysis of deformation-induced crack tip toughening in ductile single crystals by nano-indentation, Int. J. Solid Struct. 43 (24) (2006) 7358–7370.
[62] J. Amoedo, D. Lee, Modeling the uniaxial rate and temperature dependent behavior of amorphous and semicrystalline polymers, Polym. Eng. Sci. 32 (16) (1992) 1055–1065.